J Fail. Anal. and Preven. (2022) 22:1776–1786
https://doi.org/10.1007/s11668-022-01472-z

TECHNICAL ARTICLE—PEER-REVIEWED

Failure Analysis of a Welded AISI321 Steel Bleed Air Connector of an Aircraft Engine

K. Raghavendra · M. Madan · V. Venkatesh · M. Sujata · S. K. Bhaumik

Submitted: 31 May 2022 / in revised form: 30 August 2022 / Accepted: 30 August 2022 / Published online: 12 September 2022

Abstract Failure investigation was conducted on a bleed air connector of an aircraft engine that developed an opening during service. The connector was a fabricated tubular structure wherein the flanges were circumferentially welded to a bent pipe on both the ends. The flanges and the pipe were made of austenitic stainless steel AISI 321. Fractography study confirmed that the connector had failed by fatigue mechanism. Fatigue crack had initiated at one of the weld joints. The exact location of the crack initiation was at the weld-to-tube interface. After initiation, the crack had propagated into the pipe resulting in loss of material by fracture. Investigation revealed that the primary cause of fatigue crack initiation in the connector was stress concentration at the weld joint resulting from improper weld joint design. Inferior quality of weld was another factor that contributed to the failure. A detailed analysis of the failure is presented in this article and remedial measures suggested for preventing recurrence of similar failures.

Keywords Bleed air connector · AISI 321 steel · Butt weld joint · Joint design · Fatigue fracture

K. Raghavendra · M. Madan · V. Venkatesh · M. Sujata (✉) · S. K. Bhaumik
Materials Science Division, National Aerospace Laboratories, Council of Scientific and Industrial Research (CSIR), Bangalore 560017, India
e-mail: msujata@nal.res.in

Introduction

Pipelines are integral parts of aircraft engines for transportation of various fluids, namely, fuel, hydraulic/lubricating oil, and bleed air. Failures in pipelines of aeroengines disrupt fluid flow in the system with serious consequences, which jeopardise the safety of an aircraft. An aeroengine contains different types of pipes having wall thicknesses in the range 0.6–1.2 mm and lengths varying from 50 mm or less to over 1000 mm [1]. The pipelines often have several bends for facilitating optimum routing and fitment. Most of these pipelines are made of stainless steel and they invariably have welded end fittings.

Failure by fatigue mechanism is predominant in aircraft components because of the prevailing repetitive loading cycles and it accounts for about 55% of the total failures [2–4]. Welded structures, in particular, are more susceptible to fatigue failure since the fatigue strength of weld joints is markedly affected by various factors. There are several reasons for weldment failure, and these have been documented extensively in literature [3–5]. The most common causes of fatigue failures in pipelines of aircraft engines are assembly stresses and stress concentrations arising from improper weld joint design and weld defects of various kind including microstructural factors [5, 6]. Welding of thin-walled pipes/tubes is particularly challenging. In safety critical applications such as in aircraft engines, any change in geometry of the weld joint, even a tenth of a millimetre, or generation of weld defects during fabrication can have catastrophic consequences. Presence of assembly stresses in pipelines, and residual stresses in welded structures are also known to contribute to fatigue failures in austenitic stainless steels [7, 8]. Fabrication of pipelines, therefore, needs to be done in strict compliance

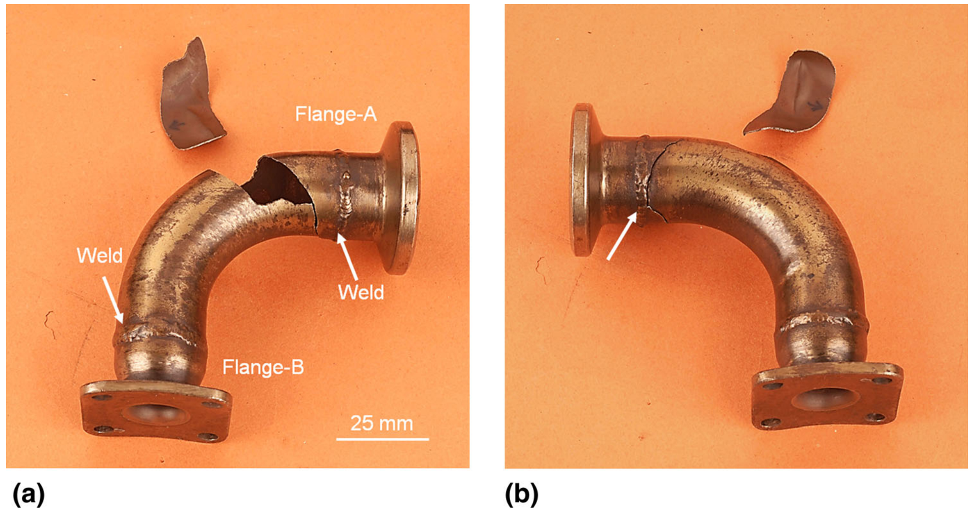

Fig. 1 (**a**) Fractured bleed air connector and the detached fragment of the pipe, and (**b**) view of the connector looking from opposite side of that in (**a**)

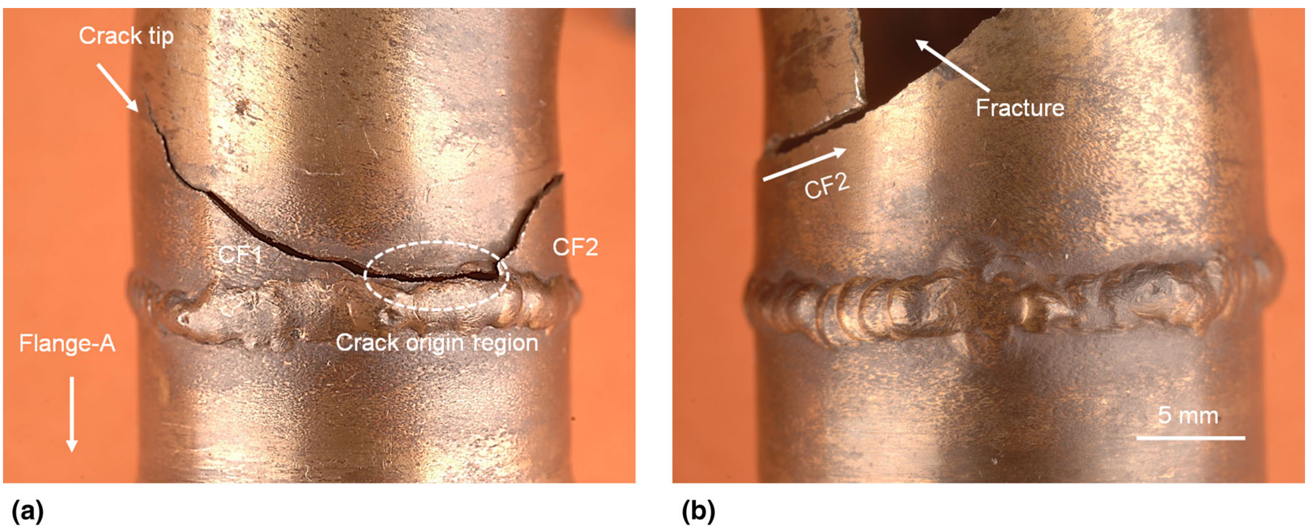

Fig. 2 (**a**) A U-shaped crack in the pipe; close-up view of the region marked by an arrow in Fig. 1b, **b** extension of CF2 leading to fracture and detachment of a fragment from the pipe of the connector

with the recommended standards to avoid failure by fatigue [9, 10].

In this article, a case study on failure of a bleed air connector of an aircraft engine is presented. The bleed air connector is part of air-conditioning system of a turboprop engine that powers a small transport aircraft. Metallurgical investigations were carried out on the failed component for identification of failure mechanism and the primary cause of failure. Based on the findings, remedial measures were suggested for prevention of similar failures.

Background Information

The bleed air connector is part of the air conditioning system of the aircraft and the air from the engine duct is used for this purpose. During operation, hot air at temperatures in the range 230–250 °C and at a pressure of 220 kPa passes through the bleed air elbow connector. At the time of failure, the connector completed a service life of 7 years and 81 days. The component does not have any specified design life and is used based on 'condition'. Failure was noticed during pre-flight servicing. The failure was in the form of an opening due to loss of material from the pipe of the connector by fracture. Subsequently, the detached fragment of the connector was recovered from the engine. The connector was fabricated by welding of flanges

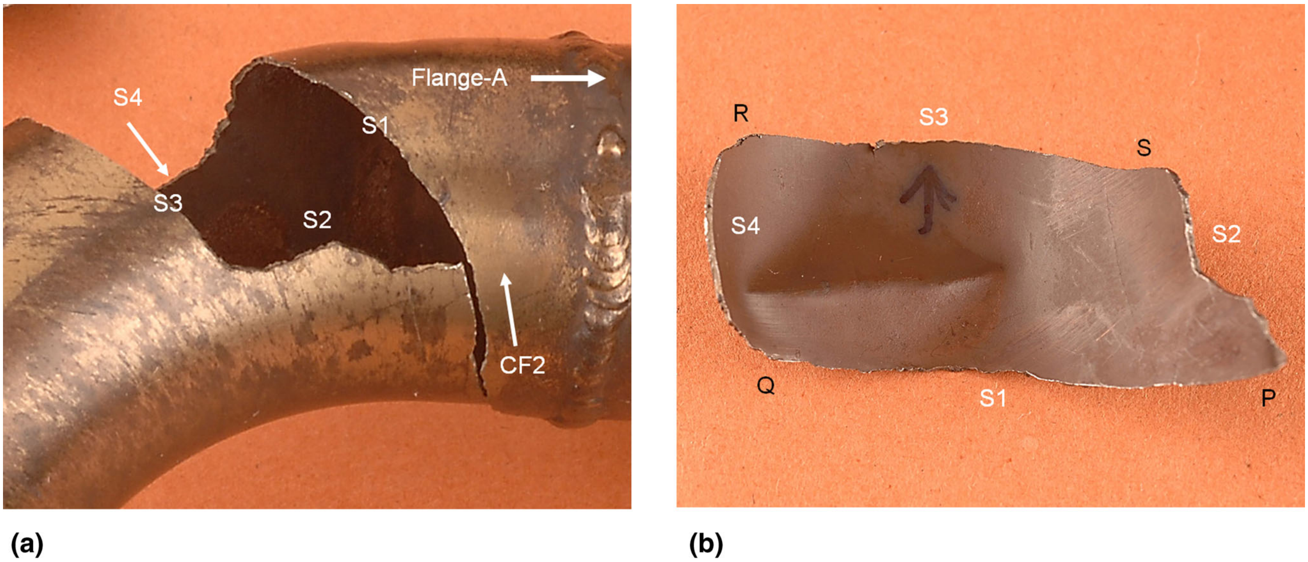

Fig. 3 (**a**) Identification of fracture surfaces on the pipe of the connector, and (**b**) corresponding mating fracture surfaces on the fragment looking from the inner surface of the pipe

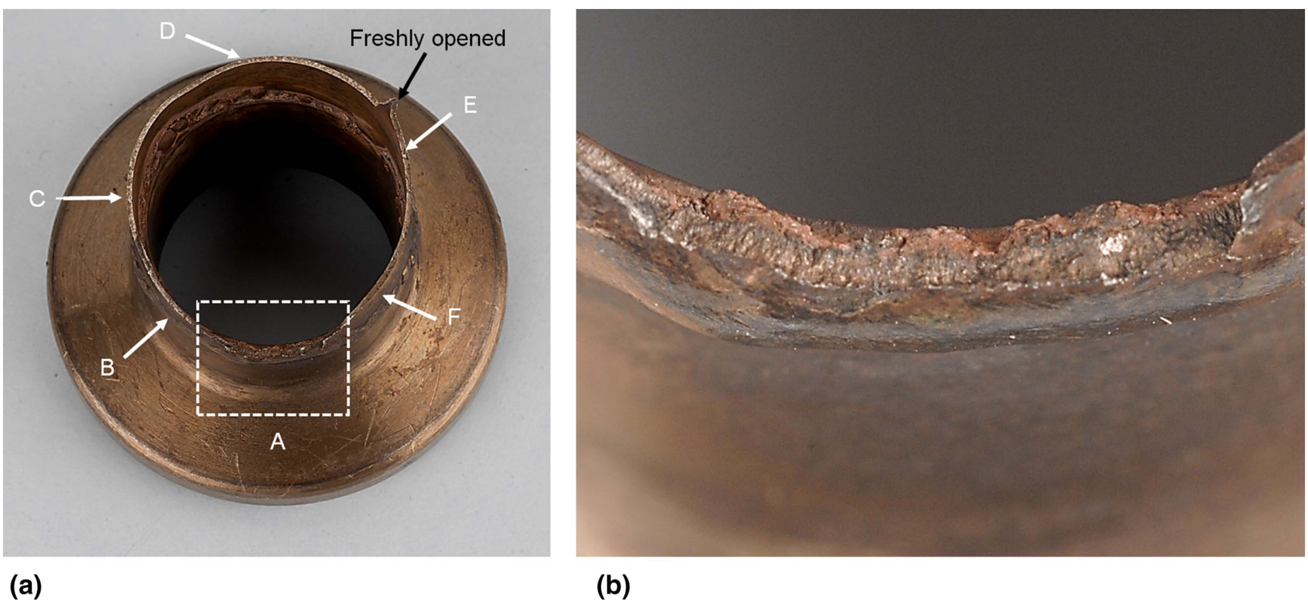

Fig. 4 (**a**) Fracture surface with Flange-A, and (**b**) magnified view of the suspected crack origin region marked in (**a**)

on either side of a bent pipe of austenitic stainless steel AISI 321.

Experimental Details

The failed bleed air connector was examined visually and under a stereo-binocular microscope (Olympus Make, Model SZX-7). Sample containing the fracture surface was sectioned from the connector and subjected to scanning electron fractography study for identification of crack origin, and the crack mechanism/propagation paths. Metallography and microstructural studies were conducted on longitudinal sections of the connector encompassing the flange, weld, and pipe for examination of type and quality of weld. Composition of material of construction of the connector was determined using an energy dispersive x-ray (EDX) analyser attached to a scanning electron microscope (SEM). Carl Zeiss-Make Model EVO18 SEM fitted with EDAX-Make EDX analyser was used for the study. Hardness survey across the weld zone was conducted using a Vickers micro-hardness tester at a load of 500 g (Leica Make, Model VMHT MOT).

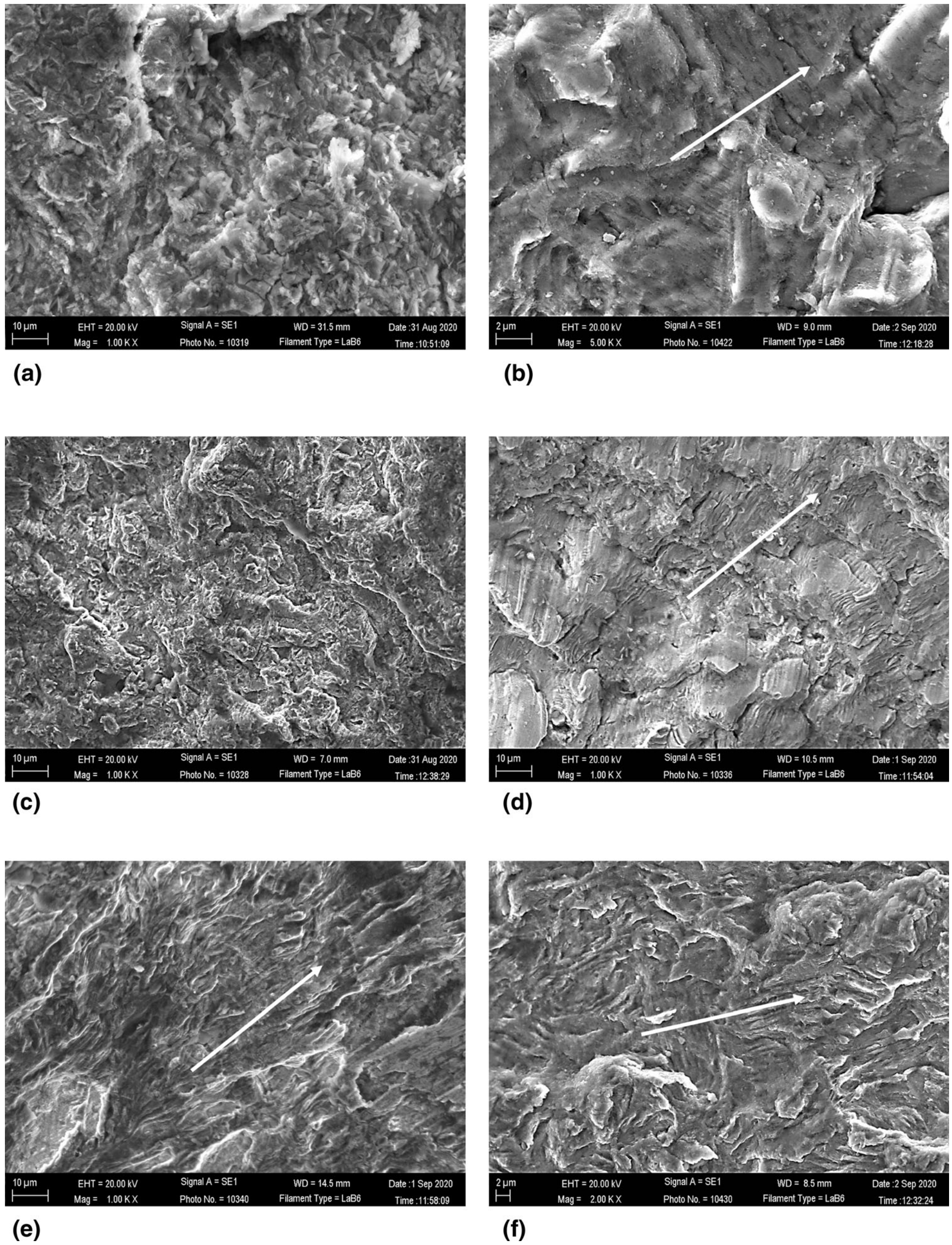

Fig. 5 (**a**–**f**) Secondary electron (SE) fractographs recorded on the regions marked 'A' through 'F' respectively in Fig. 4a showing crack arrest marks or beach marks and fatigue striations; crack propagation directions shown by arrows

Results and Discussion

Experimental Results

Description of Failure and Fracture Characteristics

The bleed air connector was fabricated by welding two flanges (designated as Flange-A and Flange-B in Fig. 1) to a bent pipe. The connector was found to have developed an opening close to Flange-A due to loss of material by fracture. Fracture occurred on the convex side of the bent pipe and the dislodged fragment exhibited roughly a rectangular shape of approximate size 35 mm × 15 mm. Figure 2a shows the close-up view of concave side of the connector, diametrically opposite to the fractured region. Examination revealed presence of a U-shaped crack in the pipe; the bottom of the crack being located at the weld. This typical profile of the crack indicated that most probably, the crack had initiated at the weld. It also appeared that after initiation, the crack had propagated on either side of the crack origin (marked as CF1 and CF2 in Fig. 2a). Further, while CF1 was still propagating into the pipe, CF2 culminated in fracture and detachment of a fragment from the pipe (Fig. 2b). Mating fracture surfaces on the pipe and the detached fragment were identified and they are marked S1 through S4 in Fig. 3.

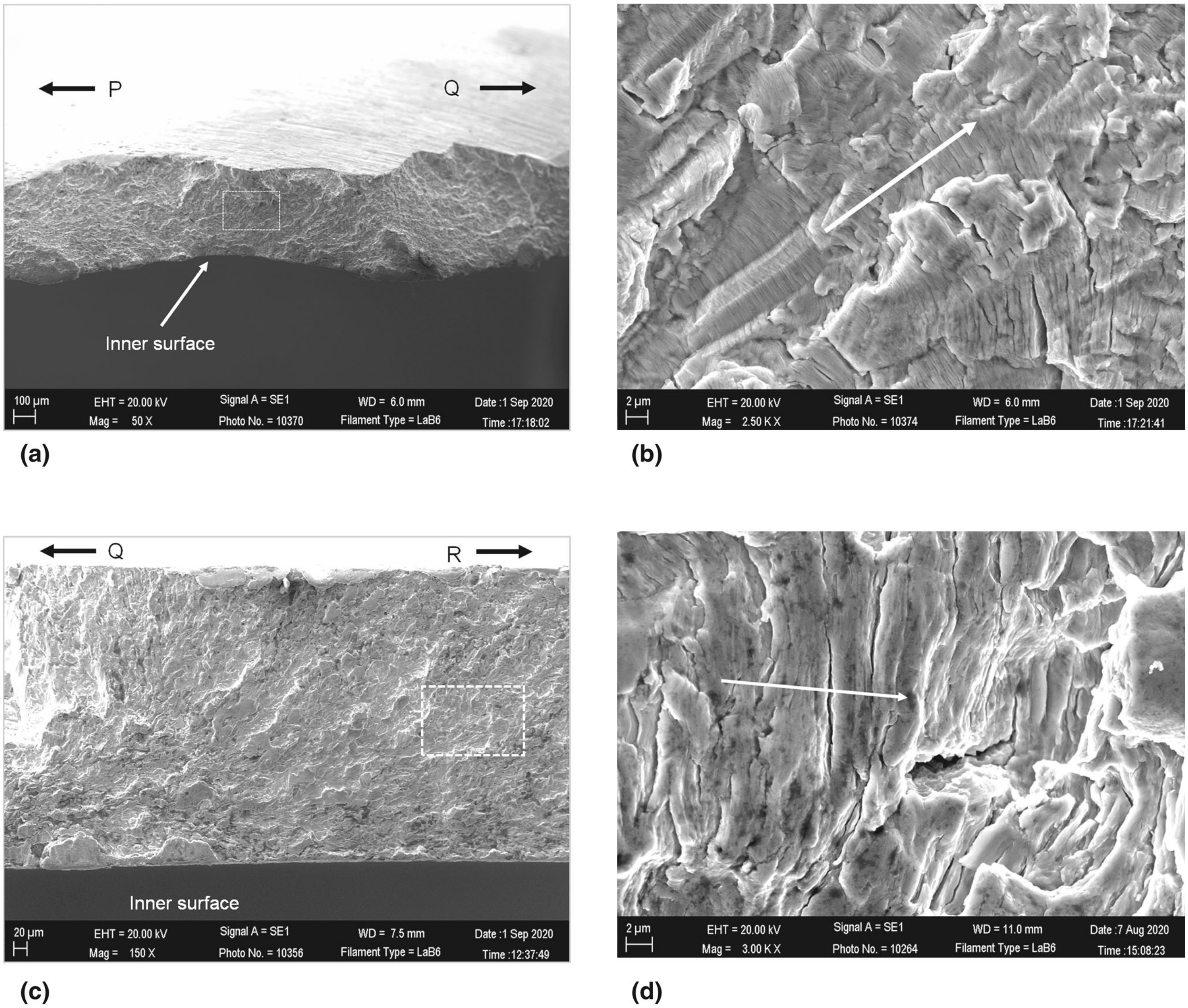

Fig. 6 SE fractographs recorded on the adjacent sides S1 (**a–b**) and S4 (**c–d**) respectively (Fig. 3b) showing crack arrest marks/beach marks, fatigue striations and local crack propagation directions; (**b**) and (**d**) magnified views of the regions marked in (**a**) and (**c**) respectively

The pipe of the connector was held together with a thin ligament between tip of CF1 and the fracture. In order to examine the fracture surface, the crack shown in Fig. 2 was pulled open and the resulting fracture surface with Flange-A is shown in Fig. 4a. Probable location of crack origin region has been marked as 'A' in Fig. 4a and close-up view of the same is shown in Fig. 4b. At this region, fracture occurred in the weld and the surface was uneven in nature. The rest of the fracture surface had a flat and relatively smooth appearance.

The entire fracture surface with Flange-A was examined under a scanning electron microscope (SEM) for identification of the crack origin and mode of crack propagation. Figure 5 shows the fractographs at locations marked 'A' through 'F' in Fig. 4a. Micro fractographic features on the fracture surface were found mostly obliterated either due to oxidation or rubbing between the mating crack surfaces. However, in isolated places, fracture features were relatively preserved, and examination of these regions confirmed fatigue mode of crack propagation; evident from the presence of crack arrest marks or beach marks and striations (Fig. 5). From the orientation of the crack arrest marks/striations, local crack propagation directions could be identified, and these have been marked by arrows on the fractographs. On superimposition of these directions on the fracture surface in Fig. 4a, it was established that on the left, crack propagation was along A → B → C → D and on the right, it was along A → F → E. This also confirms fatigue crack initiation at the weld region shown in Fig. 4b. Fractography studies were also conducted on the detached fragment of the pipe (Fig. 3b). Fractographs recorded on all four sides of the fragment are shown in Fig. 6 and 7.

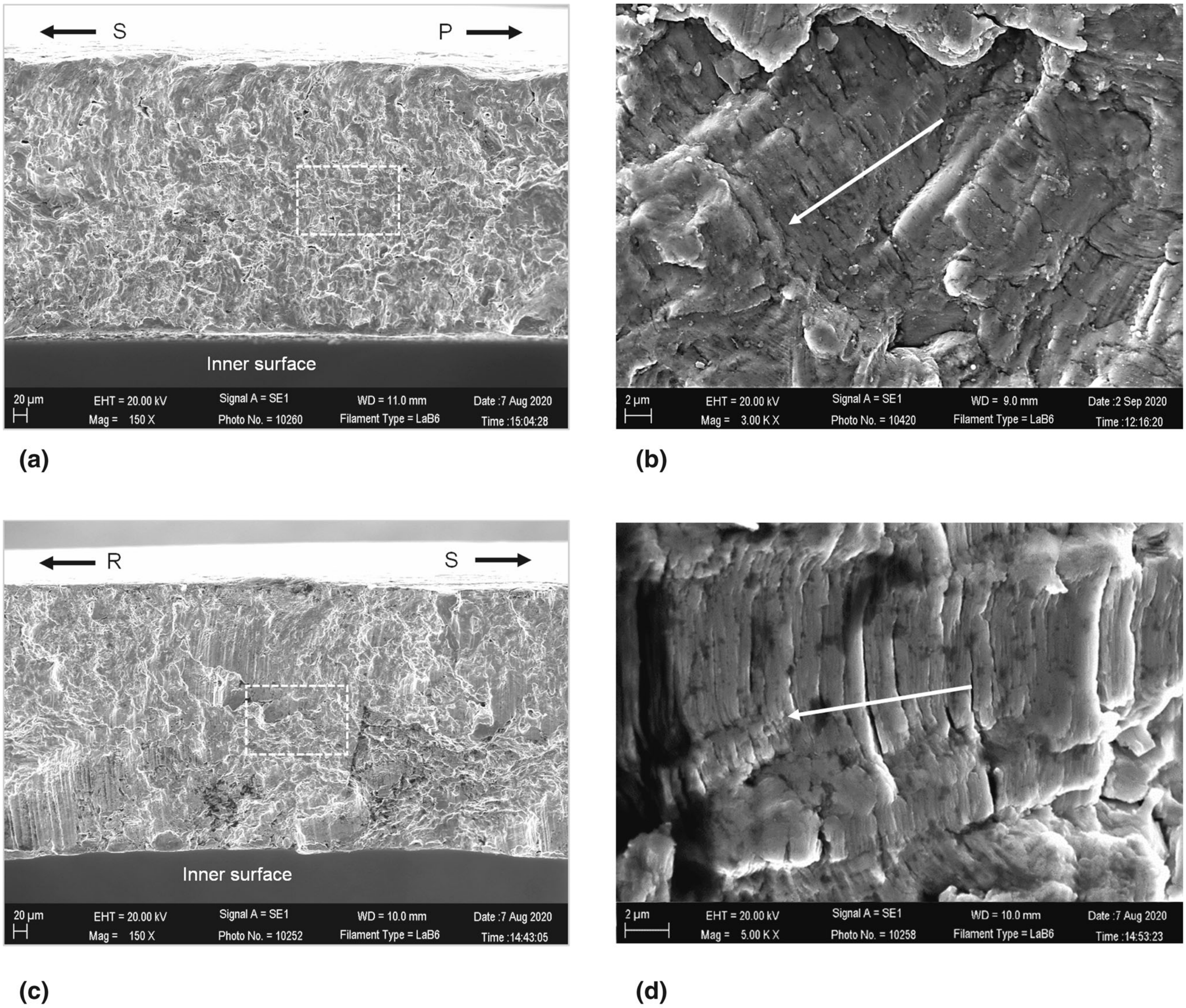

Fig. 7 SE fractographs recorded on the adjacent sides S2 (**a–b**) and S3 (**c–d**) respectively (Fig. 3b) showing crack arrest marks/beach marks, fatigue striations and local crack propagation directions; (**b**) and (**d**) magnified views of the regions marked in (**a**) and (**c**) respectively

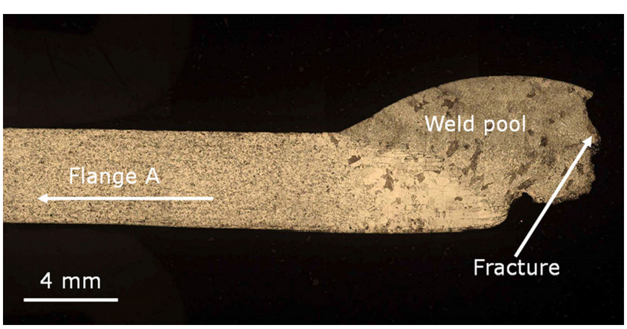

Fig. 8 Optical micrograph of a longitudinal section of the connector through fatigue crack origin showing fracture in the weld

Crack propagation directions on these sides have been marked by arrows on the fractographs. It was found that fracture in the pipe was caused due to interaction of two propagating cracks, one along P → Q → R (Fig. 6) and the other along P → S → R (Fig. 7).

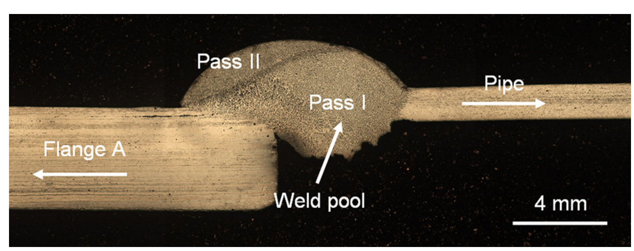

Fig. 9 Optical micrograph of a longitudinal section of the connector containing Flange-A, weld, and pipe showing misplaced weld and excess fusion zone and weld penetration

Table 1 Results of composition analysis of flange, pipe and weld material carried out by EDX analysis

Description	Composition, wt.%							
	C (Max.)	Si (Max.)	Ti (Min.)	Nb (Min.)	Cr	Mn (Max.)	Ni	Fe
AISI 321 specification	0.08	1.0	5X (%C)	…	17.0 – 19.0	2.0	9.0 – 12.0	Balance
Flange	*	0.5	0.4	…	19.0	1.7	9.1	Balance
Pipe	*	0.5	0.6	…	19.0	1.5	9.2	Balance
AISI 347 specification	0.08	1.0	…	10X(%C)	17.0 – 19.0	2.0	9.0 – 13.0	Balance
Weld	*	0.6	…	0.3	18.6	1.7	9.1	Balance

*Carbon cannot be determined accurately by EDX analysis; Max.: Maximum, and Min.: Minimum

Weld Characterization

Figure 8 shows longitudinal section of the connector through the crack origin region. The micrograph confirms initiation of fatigue crack in the weld pool. Figure 9 shows another longitudinal section of the connector containing flange-A, weld and pipe. The tubular section of the flange was joined with the pipe by butt welding. At the joint, wall-thicknesses of the flange and the pipe were approximately 4.2 mm and 1.4 mm respectively. Welding was performed in two passes. Examination revealed misplaced weld with inadequate fusion with flange-A, and excess weld penetration and fusion with the pipe.

Material of Construction

Chemical composition of material of construction of the connector was determined by EDX analyser on metallographically prepared specimens. The EDX results are given in Table 1. The EDX spectrums from the pipe and weld material are shown in Fig. 10a and b respectively. Results showed that the flange and the pipe were made of austenitic stainless steel of specification AISI 321. The composition of the weld was found conforming to AISI 347 stainless steel.

Figure 11 shows microstructures of the flange, pipe, and the weld. Microstructures of flange and pipe consisted of twinned austenite grains, typical of wrought AISI 321 steel (Fig. 11a–c). The weld pool showed presence of dendritic structure, typical of molten and solidified material (Fig. 11d). The weld structure did not show presence of any weld defects such as porosity/voids or deleterious phases. Metallurgically, no deficiencies were observed in the microstructures of flange, pipe, and weld.

Hardness survey was conducted on the longitudinal sections of the connector shown in Figs. 8, 9 and the results obtained are presented in Table 2. Hardness values determined were in the range 184–203 $HV_{0.5}$. Hardness of the weld was 15–30 points less than those of the flange/pipe. This variation in hardness was found to be within the acceptable range in welded AISI 321 steel components/structures.

Analysis of Failure

Mode of Failure and Fracture Process

Entire process of crack initiation, propagation, and fracture in the connector has been explained through schematics in Fig. 12. Fracture analysis showed that the bleed air connector has failed by fatigue mechanism. A fatigue crack had initiated at the weld between Flange-A and the pipe. After initiation, the crack had propagated through the thickness of the weld giving rise to two crack fronts. Subsequently, these two crack fronts (CF1 and CF2) had propagated into the pipe in opposite directions (Fig. 12a). The fracture and detachment of a fragment from the pipe was associated with CF2 (Fig. 12b). At some point in time during propagation of the cracks CF1 and CF2, another crack had initiated from propagating CF2 at location P (Fig. 12c). After initiation, the new crack, designated as 'CF3', had propagated along the axis of the pipe, marked as fracture plane S2. After propagating to certain distances, CF2 and CF3 had deviated their paths along fracture planes S4 and S3 respectively and formed a close loop leading to fracture and loss of a fragment from the pipe of the connector.

Fabrication of Elbow Joint

The bleed air connector was made of AISI 321 austenitic stainless steel and it was fabricated by joining two flanges on either side of a bent pipe. Joining was carried out by butt welding between the tubular section of the flanges and the central pipe having wall-thicknesses of 4.2 and 1.4 mm respectively. Welding was performed by Tungsten inert gas (TIG) welding process. The filler material used was an austenitic stainless-steel wire of grade equivalent to AISI347. Butt welding of two sections possessing such a wide difference in thickness is not a standard engineering practice owing to inherent problem of development of

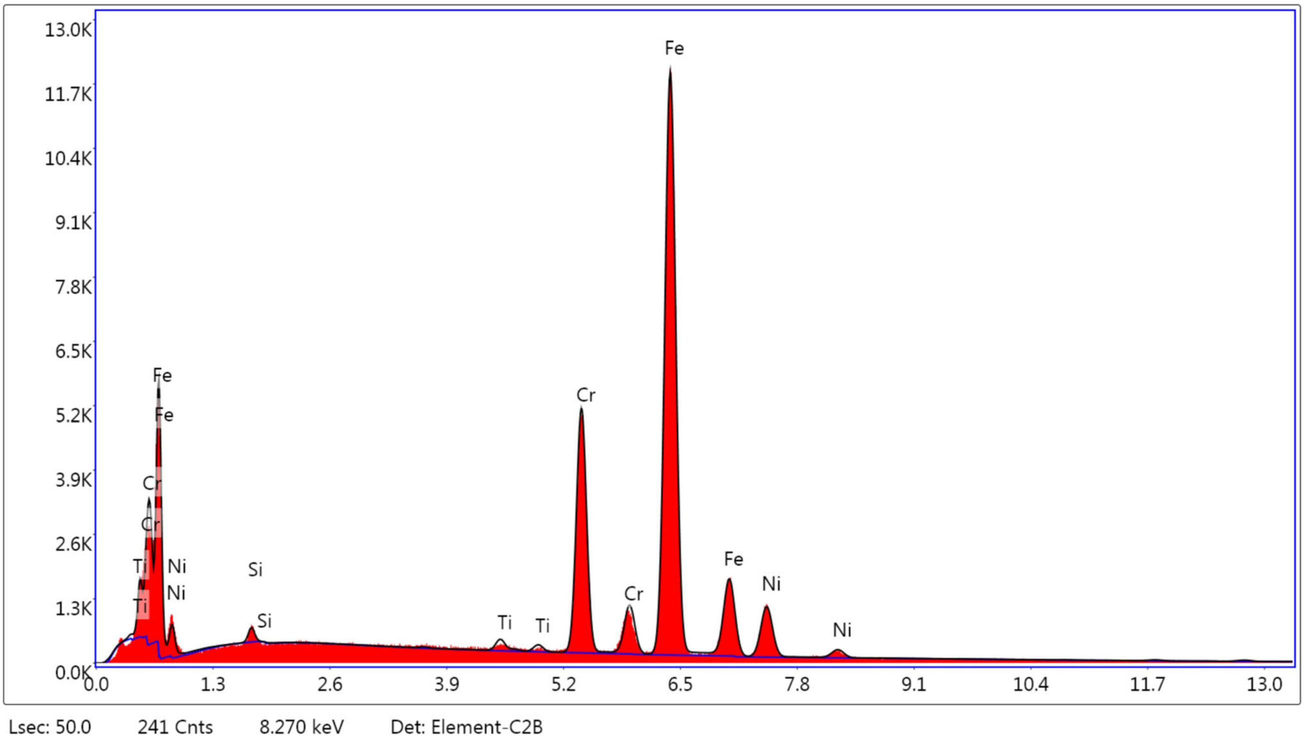

(a)

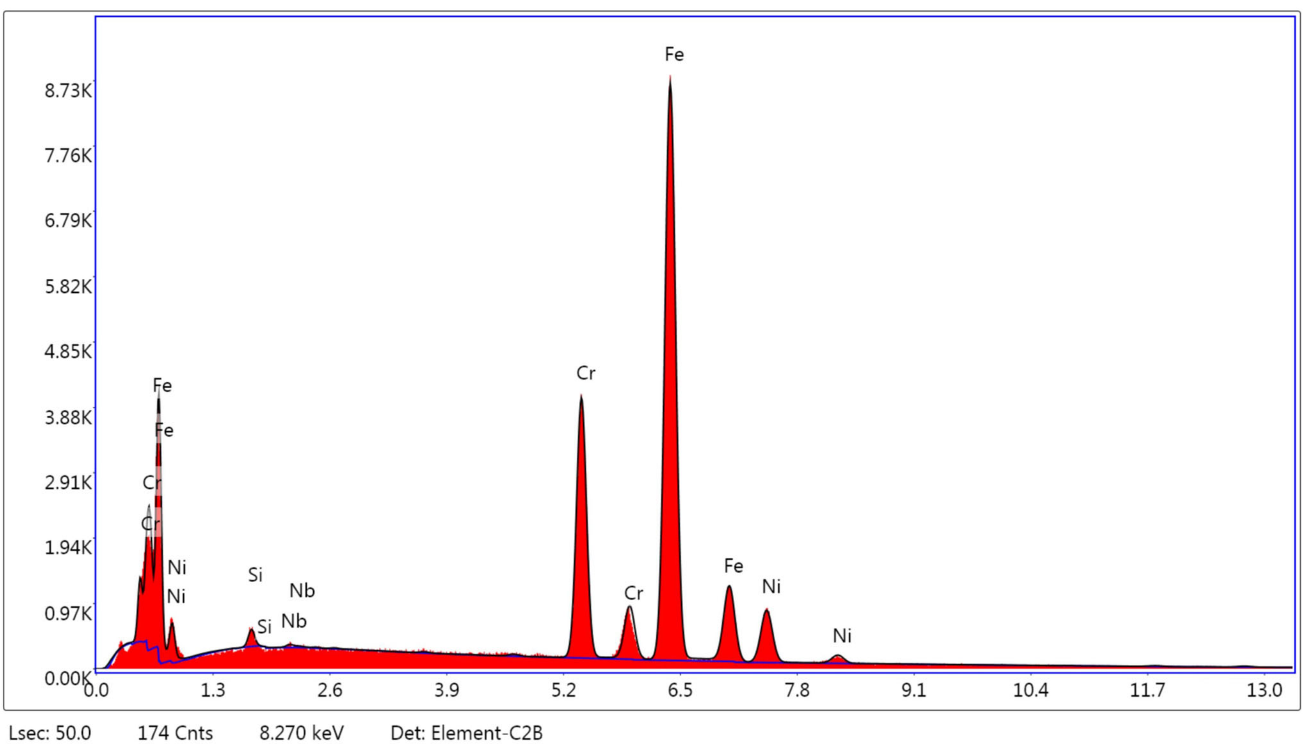

(b)

Fig. 10 EDX spectrums recorded on the (**a**) pipe and (**b**) weld region of the bleed air connector

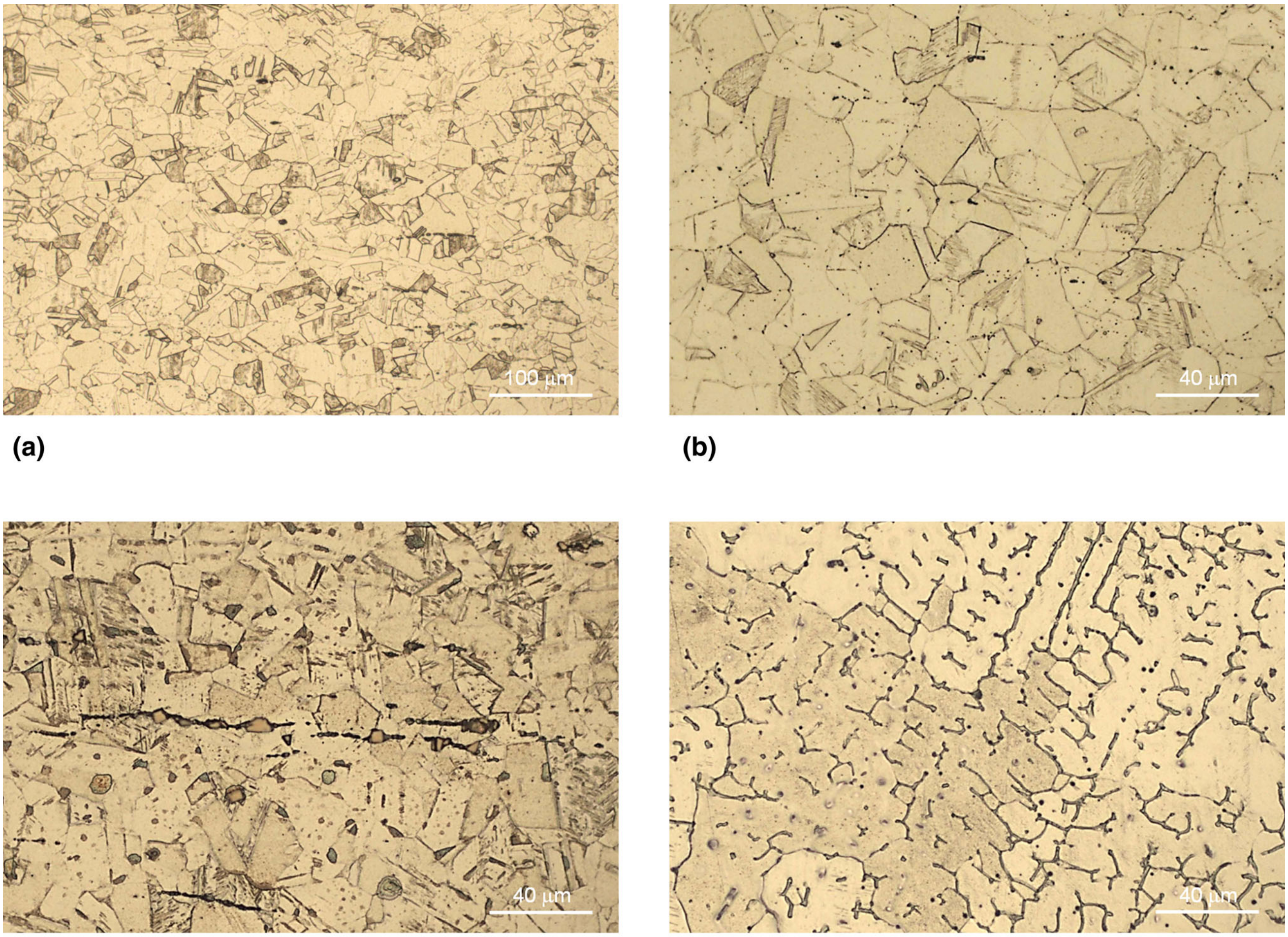

(a) (b) (c) (d)

Fig. 11 Optical microstructures of material of construction of flange, pipe, and weld: (**a–b**) flange, (**c**) pipe, and (**d**) weld

Table 2 Results of hardness survey conducted on longitudinal sections of the connector using Vickers hardness tester at a load of 500 g

	Hardness, $HV_{0.5}$	
Location	On section in Fig. 8	On section in Fig. 9
Flange	202	214
Weld	198	184
Pipe	…	203

stress concentrator at the joint arising from sudden change in geometry/dimensions (Fig. 9). Therefore, the fatigue strength of the joint reduces significantly rendering it extremely susceptible to fatigue failure [9]. When such welded structures are superimposed with assembly stresses and vibration/cyclic load, which are inevitable in the present application, the vulnerability of failure by fatigue mechanism increases many folds. To overcome this problem, the recommended practice for butt welding of two parts with a wide difference in thickness, has been beveling of the thicker part so that the slope of the surface from one part to the other is not steep. In accordance with this, the recommended fabrication scheme for bleed air connector is as shown in Fig. 13a. If not practicable, the alternative scheme is as shown in Fig. 13b.

Metallography study showed that the weld joint between the flange and pipe of the connector was inferior in quality. The weld was misplaced resulting in inadequate fusion with the flange, and there were also defects in the form of excess weld penetration and fusion in the pipe. As a result, there was undesirable weld profile at the joint resulting in severe stress concentration (Fig. 9).

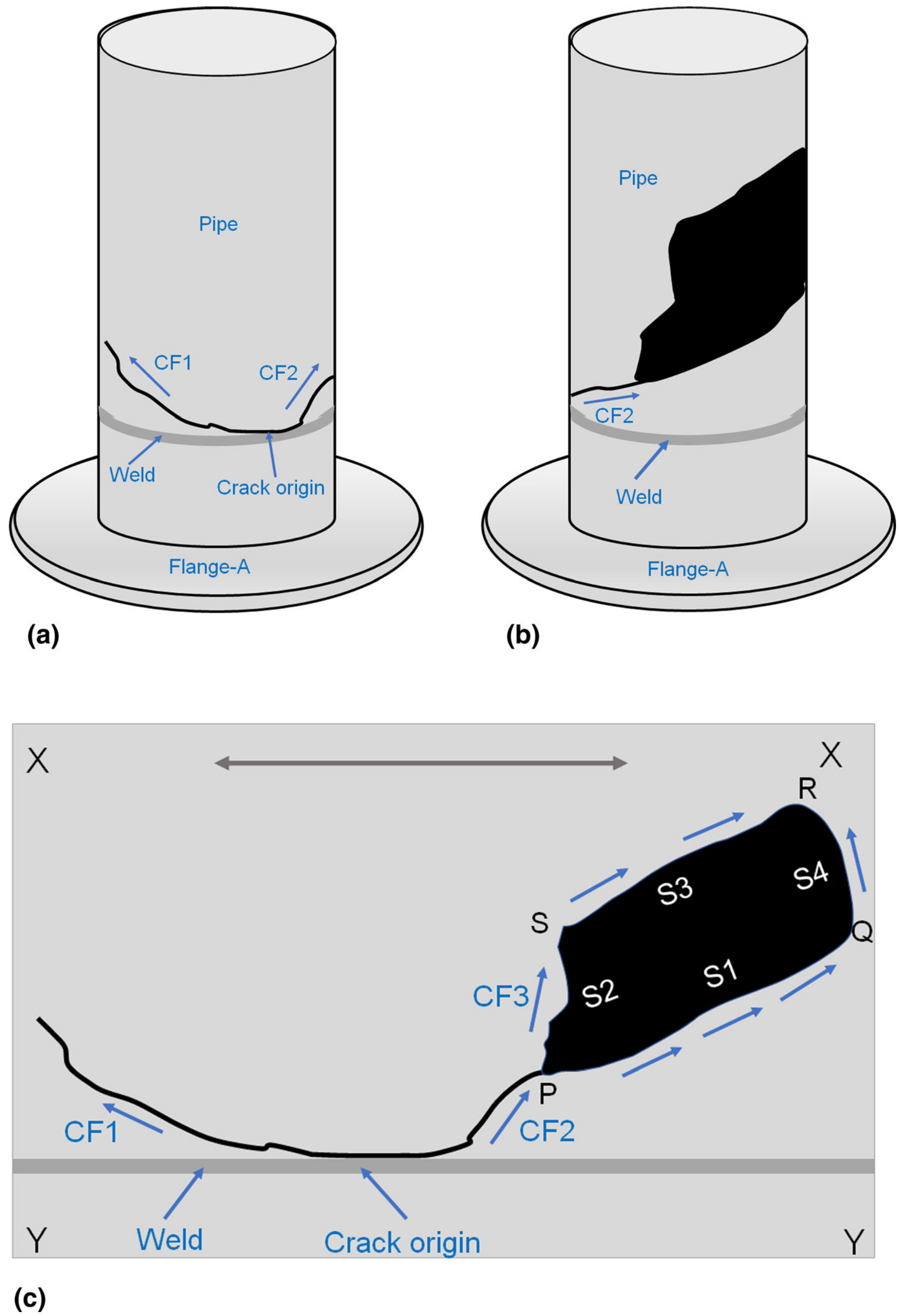

Fig. 12 Schematics showing (**a**) crack initiation at the weld joint, (**b**) extension of crack leading to fracture in the pipe, and (**c**) representation of crack initiation, propagation, and fracture on the cylindrical surface of the pipe

Primary Causes of Failure

It is evident from this investigation that the primary cause of failure of the bleed air connector was improper weld joint design between the flanges and the pipe. Butt welding of two parts having a wide difference in thickness had resulted in stress concentration with the consequence of significant reduction in fatigue strength of the joint. This had facilitated premature fatigue crack initiation at the weld. The other factor that contributed to the failure was inferior quality of weld. Fatigue crack had initiated preferentially at the weld because of combined effect of stress concentration and presence of large weld pool possessing relatively lower hardness than that of the flange/pipe.

Conclusions

The failure of a bleed air connector of air conditioning system of an aircraft was analysed. The bleed air connector that operates in the temperature range of 230 – 250 ^{0}C had

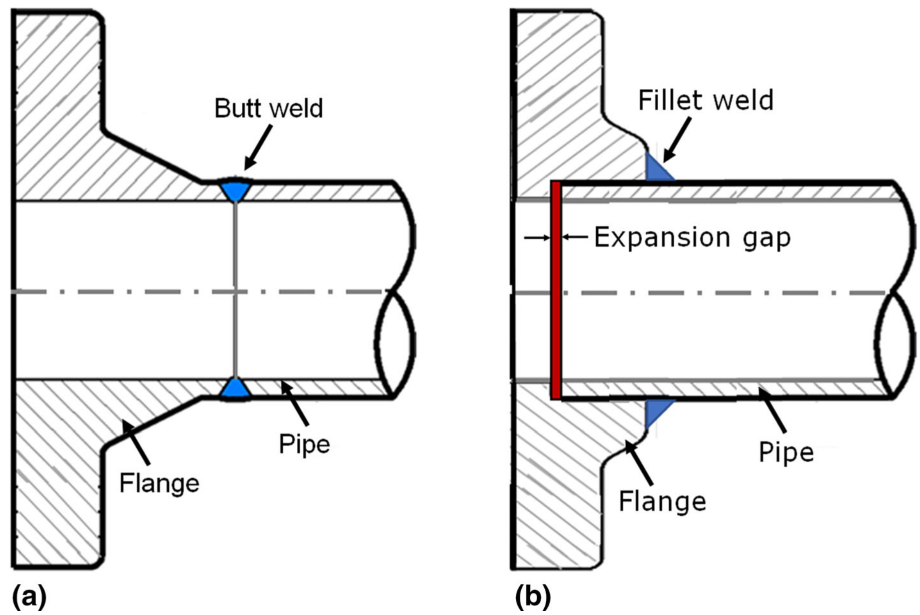

Fig. 13 Recommended practices for joining of flange and pipe having wide difference in thickness: (**a**) butt weld, and (**b**) fillet weld

failed by fatigue mechanism after a service life of 7 years and 81 days. Metallography study revealed that the joint design was improper wherein flanges and pipe with a wide difference in thickness were joined together by butt welding. This had resulted in geometrical stress concentrator and thereby, diminishing fatigue strength of the joint. The weld joint was further weakened because of inferior quality of weld. Fatigue crack had initiated preferentially in the weld because of the combined effect of stress concentration, and large weld pool with relatively lower hardness than that of the flange/pipe. Based on this investigation, modified weld joint designs for the connector have been recommended to mitigate the problems outlined.

Acknowledgments The work reported in this paper was financially supported by National Aerospace Laboratories, Council of Scientific and Industrial Research (CSIR), Bangalore, India vide Project No. M-1-298.

References

1. J.W. Dines, Welding pipes for aeroengines, Process pipe and tube welding: a guide to welding process options, techniques, equipment, NDT and codes of practice, W. Lucas, Ed., Abington Publishing, Cambridge, England, p 54–62 (1991)
2. S.J. Findlay, N.D. Harrison ND, Why aircraft fail, Materialstoday, (No.5), p 18–25 (2002)
3. A.M. Al-Mukhtar, Aircraft fuselage cracking and simulation. Procedia Struct. Integr. **28**, 124–131 (2020)
4. A.M. Al-Mukhtar, *Case studies of aircraft fuselage cracking, Advanced Engineering Forum*, vol 33 (Trans Tech Publications Ltd., Switzerland, 2019), p. 11–18
5. Failures related to welding in 'Failure analysis and prevention', W.T. Becker and R.J. Shipley (eds.), ASM Handbook, vol.11 (ASM International, Metals Park), p 156–191 (2002)
6. B. Panda, M. Sujata, M. Madan, K. Raghavendra, S.K. Bhaumik, Fatigue failure of weld joint of afterburner fuel manifold of jet engine. Eng. Failure Anal. **30**, 138–146 (2013)
7. C. Maharaj, A. Marquez, Failure analysis of a stainless steel pipe elbow in a purge gas line. J. Fail. Anal. Preven. **19**(1), 15–23 (2019)
8. C. Jang, P.-Y. Cho, M. Kim, S.-J. Oh, J.-S. Yang, Effects of microstructure and residual stress on fatigue crack growth of stainless steel narrow gap welds. Mater. Des. **31**(4), 1862–1870 (2010)
9. A. Hobbacher, Recommendations for fatigue design of welded joints and components, IIW document IIW-1823–07 ex XIII-2151r4–07/XV-1254r4–07, International Institute of Welding, p 41–107 (2008)
10. Guide to methods for assessing the acceptability of flaws in metallic structures, BS 7910:2002, British Standard, ISBN 0 580 45965 9, p 49–50